

Variations on an NHC Theme: Which Features Enhance Catalytic Transfer Hydrogenation with Ruthenium Complexes?

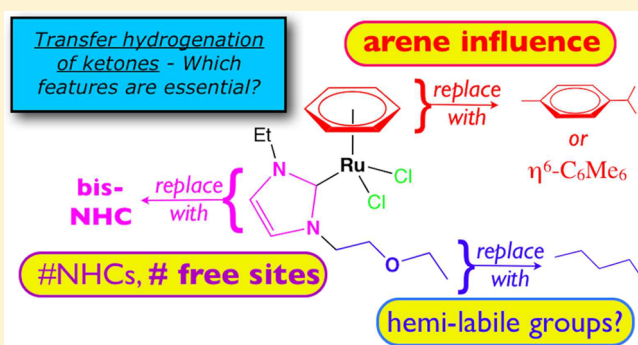
Joseph DePasquale,[†] Mukesh Kumar,[†] Matthias Zeller,[‡] and Elizabeth T. Papish^{*,†}

[†]Department of Chemistry, Drexel University, 3141 Chestnut Street, Philadelphia, Pennsylvania 19104, United States

[‡]Department of Chemistry, Youngstown University, One University Plaza, Youngstown, Ohio 44555, United States

Supporting Information

ABSTRACT: N-heterocyclic carbene (NHC) based ruthenium complexes were studied as catalysts for the transfer hydrogenation of ketones. Variations in the catalyst structure were investigated for their impact on hydrogenation and catalyst stability. Catalyst attributes included bis- or mono-NHC ligands, pendant ether groups in some cases, and arene ligands of varied bulk and donor strength. Ruthenium complexes were synthesized and fully characterized, including complexes with a monodentate NHC ligand containing a tethered ether N substituent ($\text{Im}^{\text{Et,CH}_2\text{CH}_2\text{OEt}}\text{RuCl}_2(\eta^6\text{-arene})$; arene = benzene (**4**), *p*-cymene (**5**), hexamethylbenzene (**6**)), a complex with a monodentate NHC ligand with solely alkyl N substituents ($\text{Im}^{\text{Et,Pentyl}}\text{RuCl}_2(\eta^6\text{-}p\text{-cymene})$ (**8**)), and a complex with a bis-NHC ligand ($[\text{RuCl}(\text{methylenebis}(\text{Im}^{\text{Et}})_2)(\eta^6\text{-}p\text{-cymene})]\text{PF}_6$ (**7**)) (Im = imidazole-derived NHC; superscripts indicate N substituents). X-ray crystal structures were obtained for **4**, **5**, **7**, and **8**. All of the ruthenium complexes were tested and found to be active transfer hydrogenation catalysts for the reduction of acetophenone to 1-phenylethanol in basic 2-propanol. Precatalyst **4**, which contains a tethered ether group and benzene ligand, was found to be the most active catalyst. Variable-temperature ^1H NMR studies of complexes **4**–**6** show that arene lability increases in the order $\text{C}_6\text{Me}_6 < \text{cymene} < \text{benzene}$, and this lability is directly correlated with catalytic activity. The catalysis appears to be homogeneous, and a mechanism invoking arene loss is proposed. Precatalyst **4** reduced electron-deficient ketones most easily, and 4'-nitroacetophenone was reduced under base-free conditions. The highest TOF (turnover frequency) and TON (turnover number) values obtained were 3003 h^{-1} and 845, respectively, for ketone reduction with catalyst **4**.



INTRODUCTION

Transfer hydrogenation usually requires a transition-metal catalyst, and while these frequently feature N-heterocyclic carbenes (NHCs), arenes, and pendant ether groups, it is not always clear from the literature which features are essential for catalytic activity. Transfer hydrogenation employs a “borrowing hydrogen” approach with a sacrificial donor as the hydrogen source; typical hydrogen donors include alcohols (e.g. 2-propanol) and formic acid.^{1,2} This method is often more convenient and frequently less hazardous than direct hydrogenation with H_2 gas.^{3,4} Transfer hydrogenation and direct hydrogenation have many mechanistic similarities, and usually both involve a metal hydride, a dihydride species, or a dihydrogen complex as the active catalyst.^{5–7}

The NHC ligand set has become well established in homogeneous transition-metal catalysis of many transformations,^{8–12} including direct and transfer hydrogenation. NHC ligands are frequently used in catalysis due to their strong σ -donor properties and the ease of tuning (through synthesis) the electronic and steric properties, as well as bite angles for chelates.^{8,9,12–15} NHC ligands have a remarkable advantage over tertiary phosphines in that the steric bulk and

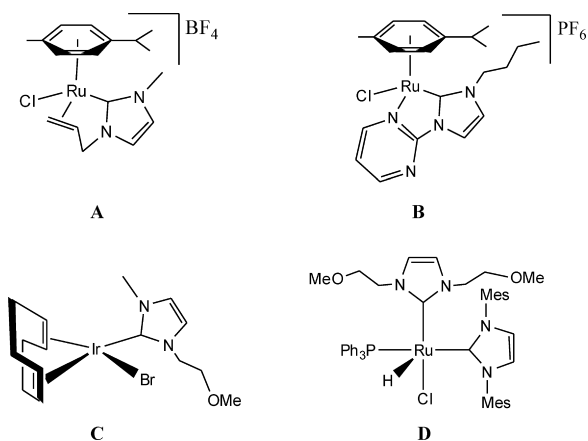
functionalities of the ligand can be altered by modification of the N substituents without causing a significant change in ligand electronics, if that is desired.⁹ Among the transfer hydrogenation catalysts with NHC ligand scaffolds, rhodium and iridium are the most commonly used metals.^{8,9,11,12,16}

Ruthenium transfer hydrogenation catalysts offer a cost advantage over rhodium and iridium,^{8,11,17} and within Ru catalysts, NHC complexes are especially promising. Various ruthenium NHC arene complexes serve as effective catalysts for the reduction of ketones,^{18–25} aldehydes,²² imines,²¹ alkenes,²⁶ and carbon dioxide.²⁷ Ester, nitro, and nitrile groups have also been reduced by transfer hydrogenation with some of these catalysts, albeit with limited success.²⁰ The NHC ligand sets employed in these $\text{Ru}(\text{NHC})(\text{arene})$ catalysts consist of mono-^{22,24} and bis-NHCs²⁷ as well as donor functionalized NHC ligands containing nitrogen,^{19,21,23} oxygen,²⁵ sulfur, or olefin donors (A; Chart 1) in the N substituent(s).^{20,26}

Hemilabile groups, in the above catalysts and in those described below, have been proposed to stabilize coordinatively

Received: June 15, 2012

Chart 1. Examples of Direct and/or Transfer Hydrogenation Catalysts with Donor Functionalized NHC Ligands^a



^aThe literature references for these complexes are as follows: A,^{20,26} B,²¹ C,³⁵ and D.³⁶

unsaturated intermediates and thereby enhance catalyst stability and efficiency.^{28–31} Recently, amine- and pyridine-derived donor groups have been chelated to Ru NHC complexes. In some cases, N donors are presumed to coordinate but structures are not available;¹⁸ in other cases, the pendant N donor has been crystallographically shown to coordinate (e.g., B; Chart 1).^{19,21} Similarly, hemilabile N and O donors have been appended to several NHC-based Ir and Rh catalysts in several cases;^{32–34} for some the enhancement of transfer hydrogenation is speculative, and for others it is well established. An experimental and computational study by Oro and co-workers showed that for square-planar Ir(I) NHC transfer hydrogenation catalysts (including C; Chart 1) the O of the pendant ether facilitates β -hydride elimination through O...H interactions rather than O to metal coordination.³⁵

Recently, Ru NHC complexes with pendant ether groups have been used for selective hydrogenation of C=C bonds (by catalyst D; Chart 1) and metathesis.^{36,37} Catalyst D does not have the ether coordinated to the metal center, but closely related complexes show ether coordination which is invoked as a mechanistic possibility.

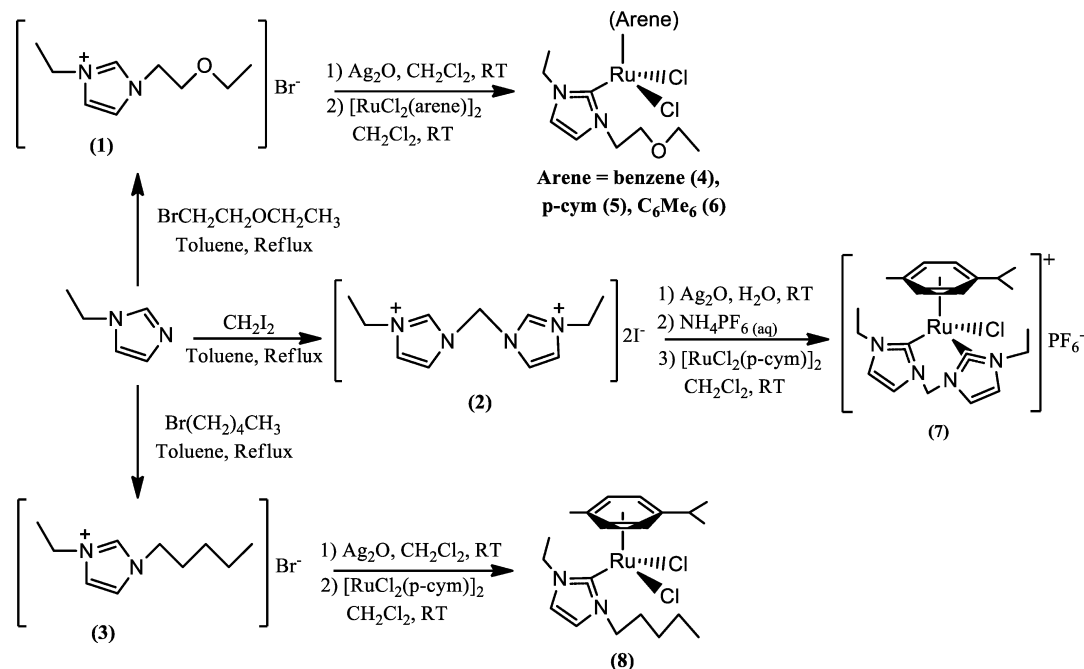
Despite the above interesting results, a careful comparison of Ru complexes with similar structures, some containing and some lacking ether groups, has not yet been done (to the best of our knowledge). In this paper we report novel ruthenium NHC complexes and investigate the roles of mono- or bis-NHC ligands, pendant ether groups, and arene ligands in determining catalyst activity for transfer hydrogenation.

RESULTS AND DISCUSSION

Synthesis and Characterization of Imidazolium NHC Ligand Precursors 1–3 and Coordination to Ru(II) To Form Complexes 4–8. In designing Ru complexes 4–8 (Scheme 1), we were interested in probing the role in catalysis of pendant ether groups and different arenes (4–6), bis- (7) vs mono-NHC (4, 5, 6, 8) ligands, and the resulting differences in charge of the complexes (all but cationic 7 are neutral). Furthermore, 5 and 8 are very closely related, only differing by O versus CH₂ in the N substituent.

Adapted literature methods^{38,39} were used to develop a divergent synthesis whereby 1-ethylimidazole could be reacted with different alkyl halides to yield three unique imidazolium bromide compounds as NHC precursors (1–3 in Scheme 1). These imidazolium salts were characterized by ¹H and ¹³C NMR and mass spectrometry. Then, 1–3 were treated with silver oxide followed by [RuCl₂(arene)]₂ (see Scheme 1 for further details) to generate Ru complexes (4–8) by transmetalation procedures similar to those in the literature.⁴⁰ These Ru complexes are air stable, were obtained in good yields (68–87%), and were characterized by spectroscopic and analytical methods (¹H and ¹³C NMR, IR, mass spectrometry, and

Scheme 1. Synthesis of Im^{Et,CH₂CH₂OEt}RuCl₂(arene) (4–6), [RuCl(methylenebis(Im^{Et})₂)(η^6 -p-cymene)]PF₆ (7), and Im^{Et,Pentyl}RuCl₂(p-cym) (8)



elemental analysis) (Figures SI-1–SI-20, Supporting Information) and by X-ray crystallography for all but **6**, as described further below.

The spectral data confirmed the structures in Scheme 1 and showed some interesting features. ^1H NMR of the Ru complexes indicated loss of the C2 imidazole protons. For complexes **4–6** and **8**, the two methylene (CH_2) groups on N in each complex give rise to four unique ^1H NMR signals (δ 3.85–4.85), which are well resolved for **4** and **8** but broadened for **5** and **6** (Figures SI-1, SI-5, SI-9, and SI-17). Similarly, the methylene bridge between the NHC rings in **7** shows two signals for diastereotopic CH protons at characteristic values²⁷ of δ 5.48 and 6.10 ($^2J_{\text{H-H}} \approx 13.5$) (Figure SI-13). The ^{13}C NMR spectra of **4–8** display signals characteristic²⁷ of carbene carbons at δ 171.73–176.82. The IR spectra of **4–8** display bands at 1408–1472 cm^{-1} which correspond to the vibrational mode (ν_{NCN}) containing the carbene carbon.¹⁸

Crystal Structures of 4, 5, 7, and 8. X-ray structures for Ru(NHC) complexes **4**, **5**, **7**, and **8** were obtained, and the structures are shown in Figures 1–4. The X-ray crystallographic

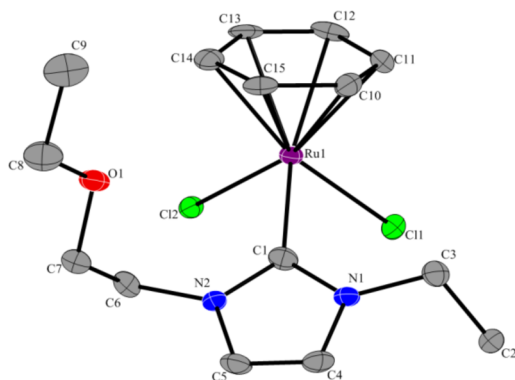


Figure 1. ORTEP diagram of $\text{Im}^{\text{Et,CH}_2\text{CH}_2\text{OEt}}\text{RuCl}_2(\text{benzene})$ (**4**). Hydrogens are omitted for clarity. Ellipsoids are shown at the 50% probability level.

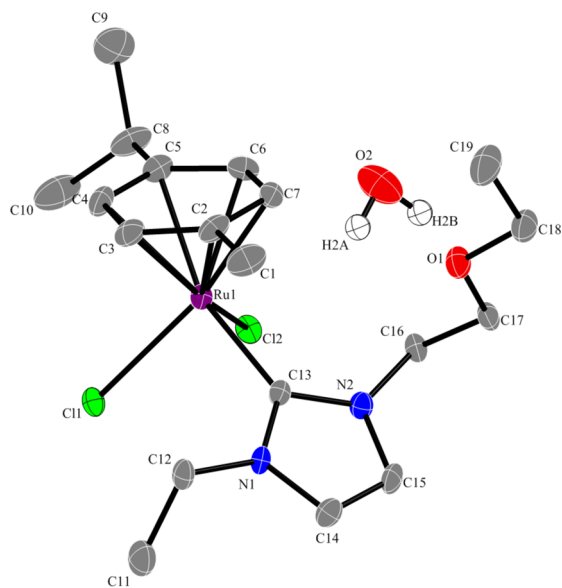


Figure 2. ORTEP diagram of $\text{Im}^{\text{Et,CH}_2\text{CH}_2\text{OEt}}\text{RuCl}_2(\text{p-cymene}) \cdot 0.9\text{H}_2\text{O}$ (**5**·0.9 H_2O). All hydrogen atoms except for those of the water molecule are omitted for clarity. Ellipsoids are shown at the 50% probability level.

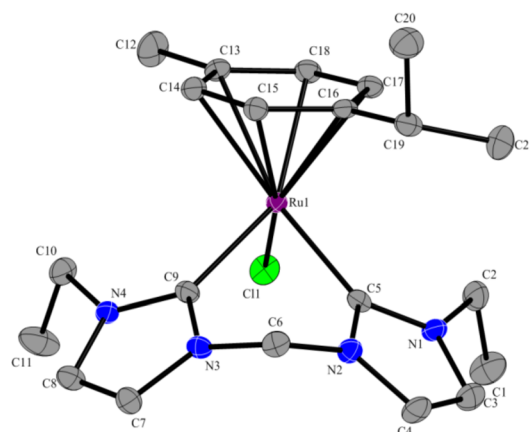


Figure 3. ORTEP diagram of $[\text{RuCl}(\text{methylenebis}(\text{Im}^{\text{Et}})_2)(\eta^6\text{-p-cymene})]\text{PF}_6$ (**7**). Hydrogens and the PF_6^- anion are omitted for clarity. Ellipsoids are shown at the 50% probability level.

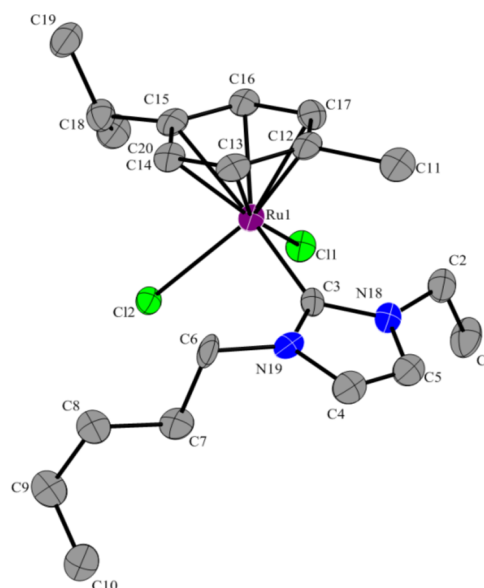
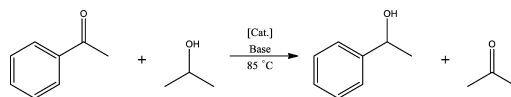


Figure 4. ORTEP diagram of $\text{Im}^{\text{Et,Pentyl}}\text{RuCl}_2(\text{p-cym})$ (**8**). Hydrogens are omitted for clarity. Ellipsoids are shown at the 50% probability level.

data and the bond lengths and angles are depicted in Table SI-3 (Supporting Information) and Table 1, respectively. All three structures feature piano-stool geometries with η^6 -arenes. The Ru–C_{carbene} and Ru–Cl bond distances and the angles in all

Table 1. Selected Bond Lengths (Å) and Angles (deg) for Complexes **4**, **5**, **7**, and **8**

	4	5 ·0.9 H_2O	7	8
Ru1–C _{carbene}	2.064(5)	2.077(4)	2.038(4), 2.044(4)	2.077(9)
Ru1–Cl1	2.421(2)	2.4396(12)	2.422(1)	2.432(2)
Ru1–Cl2	2.429(2)	2.4393(11)		2.442(2)
Ru–O	4.248(4)	4.419(4)		
Cl1–Ru1–C _{carbene}	87.06(2)	90.07(12)	89.48(1), 88.39(1)	91.1(2)
Cl2–Ru1–C _{carbene}	92.37(1)	84.71(10)		90.4(2)
Cl1–Ru1–Cl2	85.09(5)	84.75(3)		85.07(8)
C _{carbene} –Ru1–C _{carbene} (bite angle)			82.48(2)	

Table 2. Catalytic Transfer Hydrogenation of Acetophenone to 1-Phenylethanol in 2-Propanol^a

entry	cat.	C/B/S ^b	base	conversion at 1 h, % ^c	conversion, % (time, h) ^c	TOF at 1 h, h ⁻¹	TON (time, h)
1	7	1/25/100	KOH	60	91 (3)	60	91 (3)
2	7	1/25/100	KO ^t Bu	81	93 (3)	81	93 (3)
3 ^d	7	1/100/100	KO ^t Bu	78	99 (24)	78	99 (24)
4	7	1/8/100	KO ^t Bu	66	96 (3)	66	96 (3)
5	7	1/25/200	KO ^t Bu	51	81 (5)	102	162 (5)
6	5	1/25/200	KO ^t Bu	47	90 (5)	94	180 (5)
7	6	1/25/200	KO ^t Bu	42	89 (5)	84	178 (5)
8	8	1/25/200	KO ^t Bu	55	94 (5)	110	188 (5)
9	4	1/25/200	KO ^t Bu	86	94 (3)	172	188 (3)
10	4	1/25/2000	KO ^t Bu	15	42 (120)	299	845 (120)
11	4	1/0/200	KO ^t Bu	6	47 (24)	12	94 (24)
12	none	0/25/200	KO ^t Bu	3	25 (24)	N/A	N/A
13	[Ru(benz)Cl ₂] ₂ ^e	1/25/200	KO ^t Bu	35	59 (5)	70	118 (5)
14	[Ru(cym)Cl ₂] ₂ ^e	1/25/200	KO ^t Bu	47	85 (5)	94	170 (5)
15	[Ru(C ₆ Me ₆)Cl ₂] ₂ ^e	1/25/200	KO ^t Bu	40	65 (5)	80	148 (5)

^aAll reactions were carried out in 2-propanol (10 mL) at 85 °C under anhydrous and air-free conditions unless otherwise indicated. ^bC/B/S: catalyst/base/substrate. ^cConversions were determined by ¹H NMR with 1,3,5-trimethoxybenzene as internal standard and were reported as an average of two runs. ^dConditions were not anhydrous or air free. ^e2 mol of Ru supplied to form the active catalyst is presumed to correspond to 1 mol of dimer. Mole ratio of dimer to substrate was 1:400 in these entries.

four structures are unremarkable and are similar to each other and to those of ruthenium (arene) NHC complexes in the literature.^{27,40} The crystal structure of **4** has a face-to-face π - π interaction of the benzene rings (centroid distance \sim 3.4 Å)⁴¹ (Figure SI-22, Supporting Information), generating dimeric moieties in the crystal lattice.

Oxygen atoms (from water or ether groups) are noteworthy in the structures of **4** and **5**, due to hydrogen bonds or proximity to the metal. Complex **5** crystallized from dichloromethane and hexanes as a water-starved hydrate (5·0.9H₂O) (from adventitious moisture), and the water molecules hydrogen bond to one chloride ligand (O2 to Cl2 distance 3.267(5) Å). Hydrophilic and water-stable organometallic complexes have been reported previously with NHC ligands^{42,43} and can occur when steric or electronic factors prevent M-C bond hydrolysis.⁴⁴⁻⁴⁸ Complex **5** can also be prepared in a dry manner and was prepared as such for the transfer hydrogenation studies. In the structures of **4** and 5·0.9H₂O, the Ru and the oxygen of the ether group are not bound but the distances (4.248(4) and 4.419(4) Å, respectively) and the number of atoms (4) linking Ru and O suggest that Ru to O binding is possible. The orientation and flexibility of the ether group is important in case vacant site(s) become available during hydrogenation. The Ru...O distance in **4** is slightly shorter than in **5**, and perhaps the angle of this ether chain is influenced by a short contact between O and a CH group of a neighboring η^6 -benzene (O to C distance of 3.515(7) Å).

Transfer Hydrogenation of Acetophenone with Precatalysts 4-8. We were interested in how mono- vs bis-NHC complexes, pendant ether groups, and the arene ligand identity serve to influence the performance of precatalysts for transfer hydrogenation. Complexes **4-8** were all found to be active precatalysts for the transfer hydrogenation of acetophenone to 1-phenylethanol (Table 2). The bis-NHC catalyst (**7**) was used to establish the best reaction conditions with acetophenone as the model substrate. With a catalyst to base

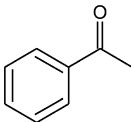
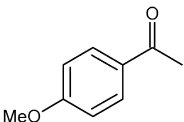
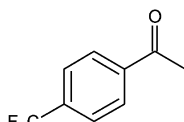
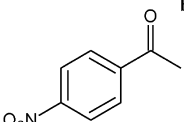
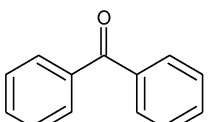
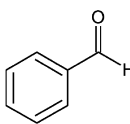
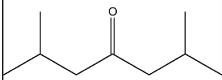
to substrate (C/B/S) ratio of 1/25/100 it was found that KO^tBu as base resulted in better initial conversion than KOH, but after 3 h both bases gave similar TON values (Table 2, entries 1 and 2).¹⁹ Upon lowering the amount of KO^tBu from a catalyst to base (C/B) ratio of 1/25 to 1/8 (Table 2, entries 2 and 4) there was a decrease in conversion after 1 h but roughly the same conversion was reached after 3 h.

The role of base is presumably for converting the precatalyst, Ru-Cl, into the expected active catalyst, Ru-H.^{5,49,50} With the bis-NHC complex **7**, attempts were made to generate a Ru-H species by the reaction of **7** with either NaOMe or KOH in methanol. In both cases the isolated complex contained a hydride peak in the ¹H NMR at δ -10.3 (Figure SI-21, Supporting Information); this chemical shift value is characteristic of ruthenium hydrides. Further characterization of this hydride complex has proven difficult, perhaps due to air and moisture sensitivity.

Lowering the amount of precatalyst **7** to 0.5 mol % (C/B/S = 1/25/200) resulted in the highest TON (162) and TOF (102 h⁻¹) values with this catalyst (Table 2, entry 5). Notably for applications in industry or in organic laboratories, precatalyst **7** demonstrated good activity in the presence of air and residual moisture (Table 2, entry 3), but reaction times required for full conversion were longer and additional base was required.

Using the optimized conditions for **7** (C/B/S ratio of 1/25/200) the monodentate NHC complexes **4-6** and **8** were tested as precatalysts (Table 2, entries 6-9). The benzene complex with a tethered ether group, **4**, showed the highest activity with a turnover frequency (TOF) and a turnover number (TON) of 172 h⁻¹ and 188, respectively (Table 2, entry 9). In 3 h over 90% conversion was reached. Catalysts **5**, **6**, and **8** required 5 h to achieve similar conversion, while the bis-NHC complex **7** falls short of 90% conversion after 5 h. The endurance of catalyst **4** was tested by increasing the C/B/S ratio to 1/25/2000 (0.05 mol % catalyst) (Table 2, entry 10), resulting in a TOF of 299 h⁻¹ at 1 h and a TON of 845 after 5 days. Without base present, catalyst **4** (0.5 mol %) showed poor activity, only

Table 3. Catalytic Transfer Hydrogenation of Carbonyl Compounds in 2-Propanol with $\text{Im}^{\text{Et,CH}_2\text{CH}_2\text{OEt}} \text{Ru}(\text{Cl})_2(\text{benzene})$ (4)^c

Entry	Substrate	Conv. ^a 1 h (%)	Conv. ^a (h) (%)	TOF (h ⁻¹) at 1h	TON (h)
1		86	94 (3h)	173	189 (3 h)
2		78	78 (3h)	156	156 (3 h)
3		98 (75 at 3 min.)		197 (3003 at 3 min.)	197 (1 h)
4		8	79 (24h)	17	158 (24 h)
5		73	88 (5h)	146	177 (5 h)
6		16	21(5h)	33	41 (5 h)
7		8	15 (5h)	17	30 (5 h)

^aConversions were determined by ¹H NMR with 1,3,5-trimethoxybenzene as internal standard and were reported as an average of two runs. ^bNo base was used because the use of KO^tBu resulted in no conversion. ^cIn every case the product formed was the expected alcohol formed by C=O reduction. C/B/S = 1/25/200. All reactions were carried out in 2-propanol (10 mL) at 85 °C.

reaching 47% conversion in 24 h (Table 2, entries 9 and 11). Without catalyst present there was significantly less formation of 1-phenylethanol: only 25% in 24 h (Table 2, entry 12).⁵¹

The structure of complex **8** is identical with that of **5**, except for a swap of O for CH₂ in one N substituent, which converts the pendant ether to an alkyl group. Both complexes have nearly identical steric profiles of their ligands, and the primary coordination geometries are virtually identical (Figures 2 and 4). The orientation of the long, five-membered-chain N substituents in complexes **5** and **8** is the major difference in the solid-state structures of these complexes (see overlay in Figure SI-23, Supporting Information). These precatalysts perform hydrogenation very similarly with nearly identical percent conversion at 1 and 5 h (Table 2, entries 6 and 8). This shows that the tethered ether group does not enhance (or harm) the activity of the catalyst.

Commercially available $[(\eta^6\text{-arene})\text{RuCl}_2]_2$ complexes were also tested as precatalysts for transfer hydrogenation (Table 2, entries 13–15). These complexes were the starting materials in the synthesis of **4**–**8**, and they are also potential decomposition products if NHC ligand loss occurs. With *p*-cymene as the arene, hydrogenation results show that the Ru dimer performs similarly to complexes **5**, **7**, and **8** (Table 2, entries 5, 6, 8, and 14). In contrast, precatalyst **6** displays a modest enhancement in activity relative to $[\text{Ru}(\text{C}_6\text{Me}_6)\text{Cl}_2]_2$ (Table 2, entries 7 and 15). With **4**, a significant enhancement in percent conversion to hydrogenated products is evident by comparing **4** to $[\text{Ru}(\text{benzene})\text{Cl}_2]_2$ (86% conversion in the first hour vs 35% conversion, and these differences remain at longer times; see Table 2, entries 9 and 13). This suggests that the NHC ligands do play an important role in the active catalyst.

In conclusion, a monodentate NHC ligand combined with benzene as the arene (**4**) appears to give the best hydro-

generation catalyst in this study, and while this complex does contain a pendant ether group, it does not appear to enhance catalytic rates.

Transfer Hydrogenation of Other Carbonyl Substrates with Precatalyst 4. The most active precatalyst (**4**) for the transfer hydrogenation was used to investigate substrate scope (Table 3). Electronic effects were investigated by using aryl ketones with either electron-donating (OMe) or -withdrawing groups (NO₂, CF₃) in the para position (Table 3, entries 1–4). The electron-rich substrate 4'-methoxyacetophenone (Table 3, entries 1 and 2) results in decreased product formation (78% at both 1 and 3 h), suggesting that hydride transfer is slow in this case or perhaps catalyst inhibition occurs. With the σ electron withdrawing CF₃ group (Table 3, entry 3), significant rate enhancement was obtained, with 75% conversion to alcohol being observed after just 3 min (TOF of 3003 h⁻¹) and 98% conversion at 1 h. Thus, catalyst **4** is comparable to industrial catalysts with this substrate.⁵² The increased electrophilicity of the carbonyl group appears to speed up hydride attack by the active catalyst. Similar trends relating substrate electronics to catalytic rate have been observed with other transfer hydrogenation catalysts.^{53–55}

The substrate 4'-nitroacetophenone appears to be incompatible with base, as catalyst **4** led to 0% conversion at 1 and 5 h using our standard conditions. In the absence of base, 4'-nitroacetophenone was converted to the corresponding alcohol (and nitro group reduction was not observed), albeit with low activity (Table 3, entry 4). This is not surprising, as formation of the catalytically active species should be slow without base.^{56,57} To our knowledge, this is a rare example^{58–62} of base-free transfer hydrogenation without a preformed hydride ligand or internal base.^{63–71} The enhanced base-free activity of 4'-nitroacetophenone vs acetophenone (Table 2, entry 11, and Table 3, entry 4) shows that increased electrophilicity of the carbonyl group once again leads to higher activity.

The substrate benzophenone (Table 3, entry 5) illustrates that steric bulk plays a minimal role in this reaction, with 88% conversion after 5 h and only slightly depressed (cf. acetophenone) TON and TOF values. The extent of benzaldehyde hydrogenation was low (Table 3, entry 6), but there was no evidence of the Tishchenko reaction, which can occur with aldehydes in the presence of alkoxide bases.⁷² In one example, the aliphatic ketone 2,6-dimethyl-4-heptanone (Table 3, entry 7) appears to be a poor substrate, with only 15% conversion after 5 h. In summary, catalyst **4** is best suited for hydrogenation of aromatic ketones with electron-withdrawing groups.

Comparison to Phosphine Catalysts in the Literature.

The transfer hydrogenation activity of the Ru(arene)Cl₂(mono-NHC) precatalysts **4**, **5**, and **8** can be compared to that of similar Ru(arene)Cl₂(monophosphine) complexes in the literature. With arene = *p*-cymene, catalysts **5** and **8** outperformed or had activity similar to that of catalysts containing (R)-Monophos⁷³ or PPhArR (R = Me, *i*-Pr, OMe, CH₂TMS; Ar = 1-naphthyl, 9-phenanthryl, 2-biphenyl)⁷⁴ under similar conditions. However, inclusion of PPh₃ produces a superior catalyst, as the precatalyst Ru(arene)Cl₂PPh₃ (arene = *p*-cymene, benzene) hydrogenates acetophenone with 93% conversion in 10 min (C/KO^tBu/acetophenone = 1/5/200). This is significantly better than results obtained with our best precatalyst, **4** (Table 2, entry 9).⁷³

Distinguishing Homogeneous vs Heterogeneous Catalysis. We investigated whether these catalysts remain

homogeneous or form heterogeneous catalysts in situ. Mercury tends to coat nanoparticles, and mercury inhibition of a reaction suggests a heterogeneous catalyst.^{75–78} The mercury test with precatalyst **4** and acetophenone in basic 2-propanol showed no significant inhibition of conversion to products (Table 4). Precatalysts **5–8** were also tested with Hg, and it

Table 4. Mercury Test for the Catalytic Transfer Hydrogenation of Acetophenone to 1-Phenylethanol in 2-Propanol with Catalyst 4^a

entry	4/Hg ⁰	conversion, %		
		5 min ^b	1 h ^b	3 h ^b
1	1/0	33	86	94
2	1/300	n.d.	84	94

^aAll reactions were carried out in 2-propanol at 85 °C under anhydrous and air-free conditions. 4/KO^tBu/acetophenone = 1/25/200. The normal reaction procedure was used as detailed in the Experimental Section, with the only exception being that Hg⁰ was added after 5 min of reaction time. ^bConversions were determined by ¹H NMR with 1,3,5-trimethoxybenzene as internal standard and were reported as an average of two runs; n.d. = not determined.

was found that the *catalytic activity did not decrease* with any of the complexes (Table SI-1, Supporting Information). Thus, the Hg test suggests that **4–8** are *homogeneous, molecular catalysts*.

Furthermore, Finke et al. have shown that quantitative poisoning can also distinguish small molecular clusters vs nanoparticle catalysts (this was used to identify a Rh₄ cluster as the active benzene hydrogenation catalyst, rather than a nanoparticle).^{79,80} If 1 equiv or less of a poison (e.g. 1,10-phenanthroline) is spiked into a reaction mixture, this should effectively poison a nanoparticle catalyst where far less than 1 equiv of metal atoms is on the surface and accessible. However, for a molecular catalyst all metal atoms are accessible and this quantity of poison may slow down catalysis, but it will not shut down catalysis completely.^{79,80} We attempted to poison catalyst **4** in a similar fashion. The poison, 1,10-phenanthroline, was added to a standard reaction mixture containing **4** after 5 min (as suggested by Finke et al., the poison is added after the reaction has started so that the active catalyst is present). With 1 equiv of poison, reaction still occurs with only a 9% decrease in percent conversion (Table 5). Similarly, even 5 equiv of

Table 5. Quantitative Poisoning Study with 1,10-Phenanthroline for the Catalytic Transfer Hydrogenation of Acetophenone to 1-Phenylethanol in 2-Propanol with Catalyst 4^a

entry	1,10-phenanthroline/4	conversion, %	
		5 min ^b	1 h ^b
1	0/1	33	86
2	1/1	n.d.	77
3	5/1	n.d.	60

^aAll reactions were carried out in 2-propanol at 85 °C under anhydrous and air-free conditions. 4/KO^tBu/acetophenone = 1/25/200. The normal reaction procedure was used as detailed in the Experimental Section, with the only exception being that 1,10-phenanthroline is added as a mixture in 1 mL of 2-propanol after 5 min of reaction time, bringing the final volume to 10 mL. ^bConversions were determined by ¹H NMR with 1,3,5-trimethoxybenzene as internal standard and were reported as an average of two runs; n.d. = not determined.

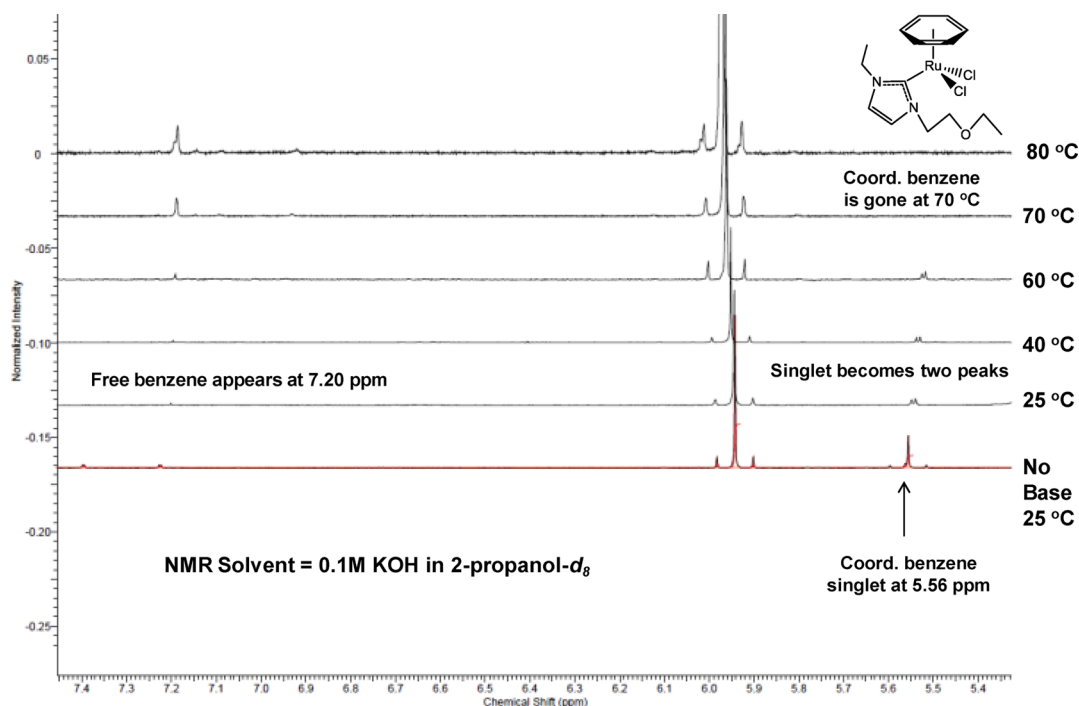


Figure 5. Temperature-dependent ^1H NMR spectra for complex **4** upon addition of base in 2-propanol- d_8 . Between acquisition of the first and second spectrum at 25 °C base was added. These conditions are similar to those used for catalysis (85 °C), but no substrate is present.

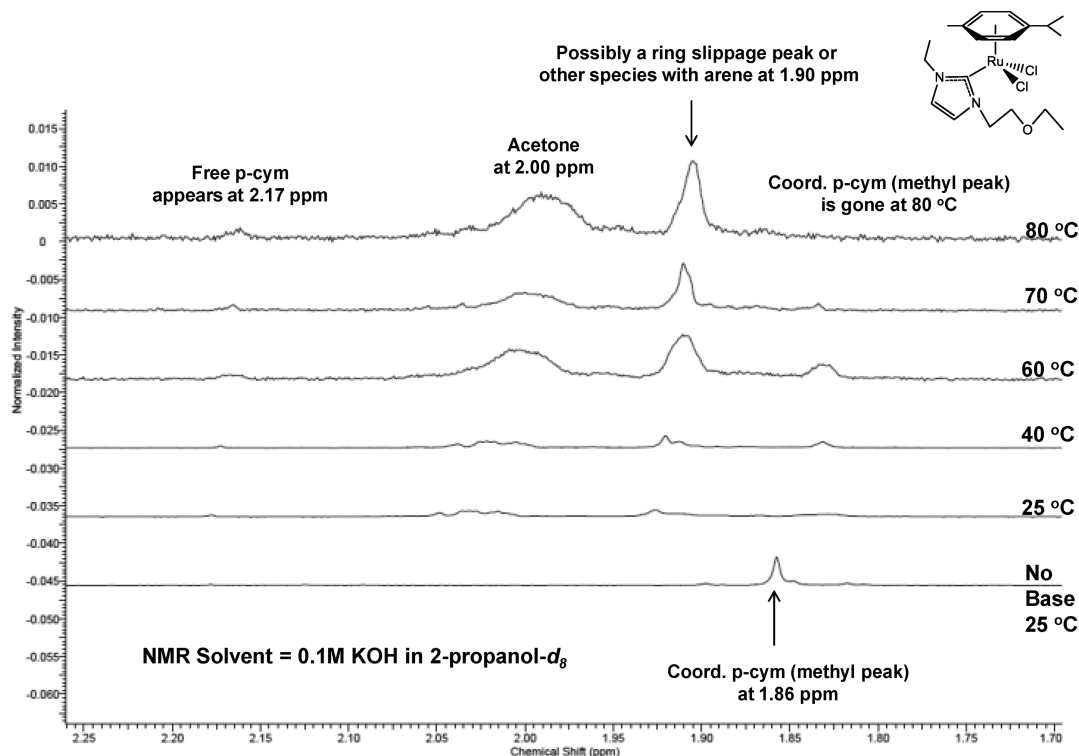


Figure 6. Temperature-dependent ^1H NMR spectra for complex **5** upon addition of base in 2-propanol- d_8 . Between acquisition of the first and second spectrum at 25 °C base was added. These conditions are similar to those used for catalysis (85 °C), but no substrate is present.

poison only leads to a 26% decrease in activity. In the literature,^{79,80} these relative quantities of poison are known to stop product formation completely when authentic nanoparticles are used as a heterogeneous catalyst. These poisoning experiments, combined with the Hg test, indicate that **4** is most likely a homogeneous catalyst.

Variable-Temperature Studies of 4–6 in Basic 2-Propanol without Substrate. This study began as an attempt to explain why transfer hydrogenation is much faster (in the first hour) with **4** in comparison with precatalysts **5** and **6** (Table 2, entries 6, 7, and 9). These catalysts differ only in the identity of the arene ligand (benzene (**4**), *p*-cymene (**5**), and

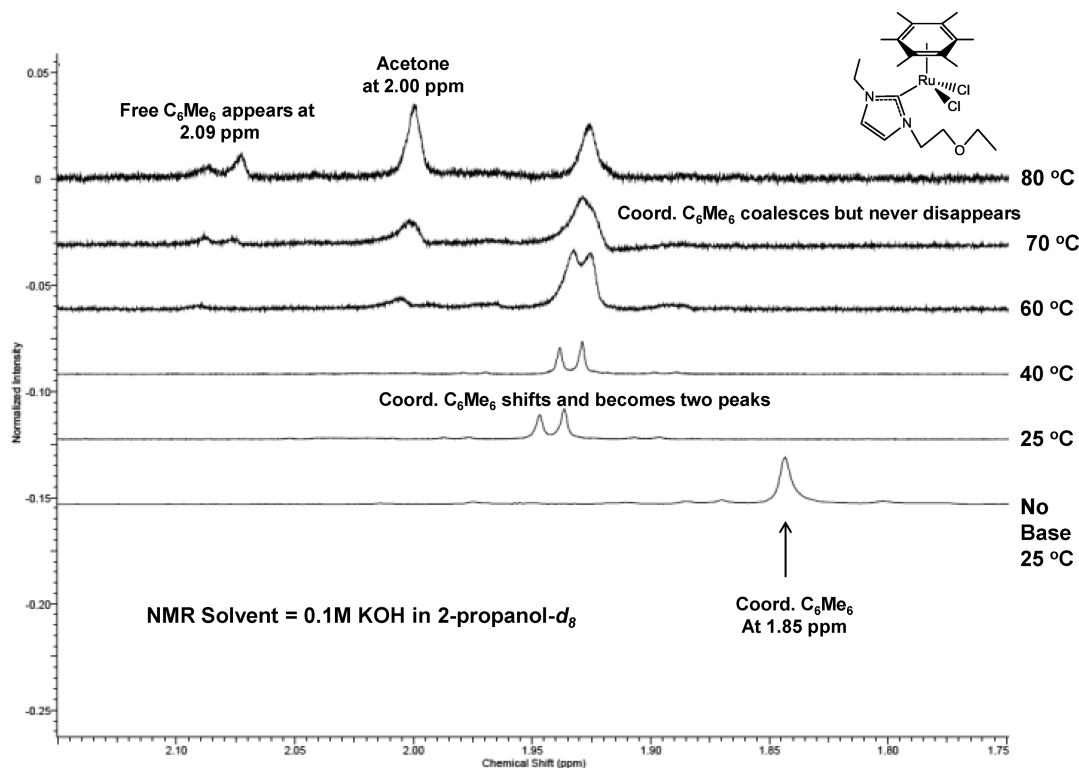


Figure 7. Temperature-dependent ^1H NMR spectra for complex **6** upon addition of base in 2-propanol- d_8 . Between acquisition of the first and second spectrum at 25 °C base was added. These conditions are similar to those used for catalysis (85 °C), but no substrate is present.

hexamethylbenzene (**6**). Since benzene is the weakest π donor, we hypothesized that an arene loss or a ring slip occurs to form the active catalyst.

Precatalysts **4–6** were studied by ^1H NMR under catalytic conditions but without substrate ($C/B = 1/10$ ($B = \text{KOH}$), 25–80 °C, 2-propanol- d_8 as solvent). Although the quality of the ^1H NMR data collected was limited by the poor solubility of the Ru(NHC) complexes in 2-propanol- d_8 at low temperatures, structural information on the catalyst was still obtained. It was found that free arene ligand formed with all complexes (Figures 5–7). The temperature at which the resonances for free arene appeared and coordinated arene diminished (and the extent of decooordination) varied among the three complexes (Table 6 and Figures 5–7).

With complex **4**, the signal for the coordinated benzene (δ 5.56) went from one singlet to either two singlets or one doublet in the presence of KOH, and furthermore as the temperature of this solution was increased the coordinated benzene signals decreased in intensity and were completely absent at 70 °C. The two peaks that formed could represent splitting of the arene hydrogens by a hydride ligand or the presence of two different species with arene coordinated, or the arene ligand could have undergone a ring slip (η^4) to give inequivalent arene ring hydrogens that produce a splitting. Ruthenium arene complexes with bent arene ligands have been observed before, e.g. $[\text{Ru}(\eta^4\text{-benzene})(\eta^6\text{-benzene})]$, and the η^4 -benzene ring does produce a similar splitting pattern.⁸¹ Free benzene (δ 7.20) was observed in the ^1H NMR upon the addition of base at 25 °C, and this peak increased in intensity as the temperature was increased (Figure 5). It is important to note that transfer hydrogenation reactions are conducted at 85 °C, and therefore, benzene loss is proposed in the active catalyst.

Table 6. Summary of Variable-Temperature NMR Study of 4–6^a

complex	arene	temp at which free arene (trace) is present, °C	What happens to the coordinated arene?
4	benzene	25	by 70 °C arene is completely uncoordinated
5	<i>p</i> -cymene	25–40	gone at 80 °C (but ring-slipped arene complex or some other complex with arene present)
6	C_6Me_6	60	still present at 80 °C along with what is potentially ring-slipped arene complex or some other complex with arene present

^aNMR tube experiments were done in 2-propanol- d_8 as solvent in the presence of 1,3,5-trimethoxybenzene as internal standard and KOH as base ($C/B = 1/10$). All NMR spectra were referenced to the methoxy protons (δ 3.62 ppm) of the internal standard (1,3,5-trimethoxybenzene). The NMR sample was degassed and flame-sealed prior to analysis.

The aromatic portion of the ^1H NMR spectra for complex **5** is complicated, but analysis of the methyl resonance of the *p*-cymene ligand shows decooordination of the arene (Figure 6), but to a lesser extent than with benzene. The peak of the methyl hydrogen atoms of the coordinated *p*-cymene is at δ 1.86 ppm before the introduction of KOH but shifts and broadens considerably after addition of base and is not detectable at 80 °C. Free *p*-cymene (δ 2.17) does not appear as a discernible peak until 70 °C, and this resonance is small and broad. There is an additional peak at δ 1.90 that forms after the addition of base which increases in intensity with increasing temperature; this peak could be attributed to a ring-slipped *p*-cymene or similar species. If we presume that a ring slip has

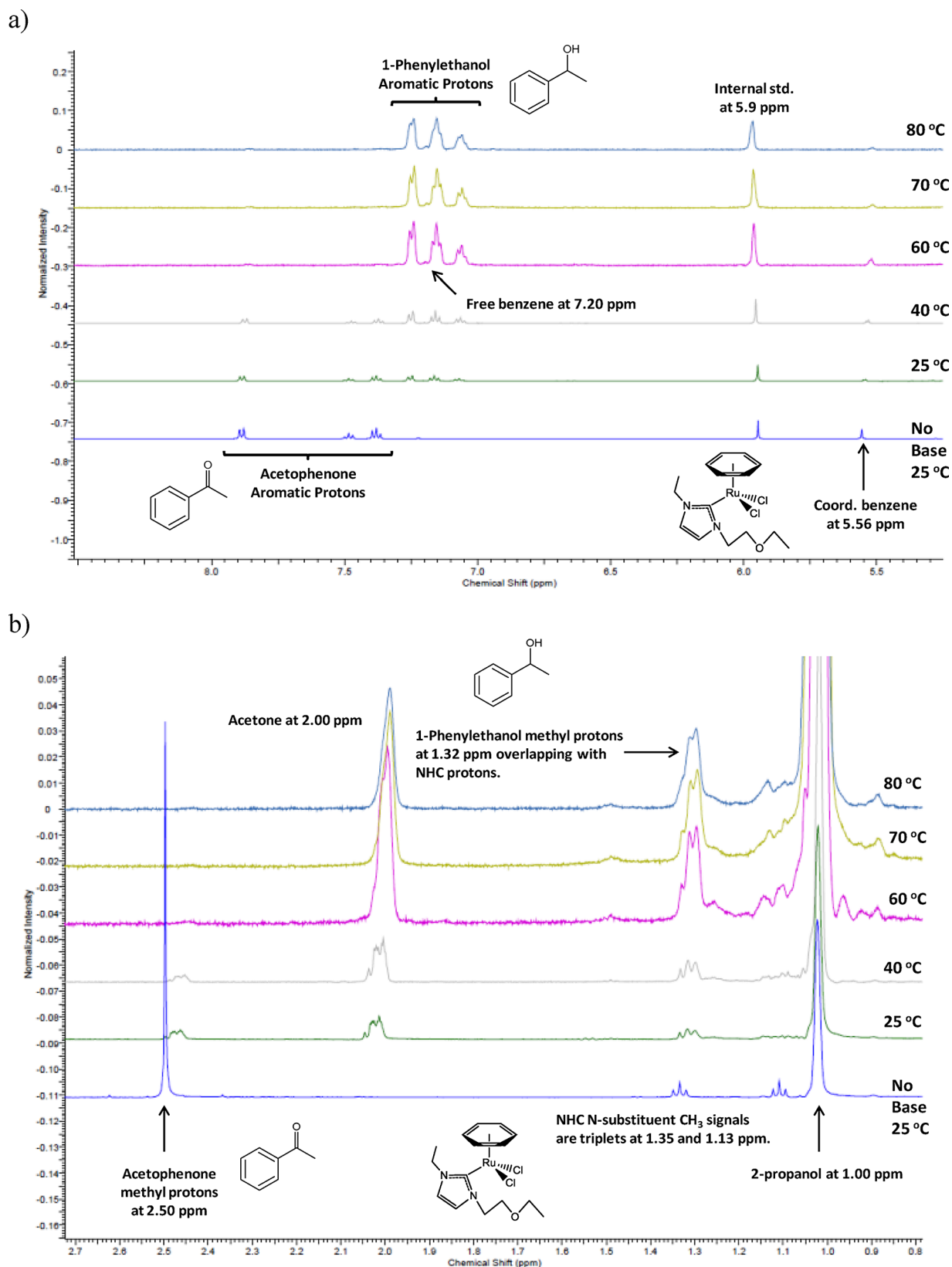


Figure 8. Temperature-dependent ^1H NMR spectra are shown for complex **4** upon addition of base in 2-propanol- d_8 : (a) δ 5.0–9.0 region; (b) δ 0.8–2.7 region. Between acquisition of the first and second spectrum at 25 °C base was added. Acetophenone as substrate was present in this study. 4/KOH/acetophenone = 1/10/10.

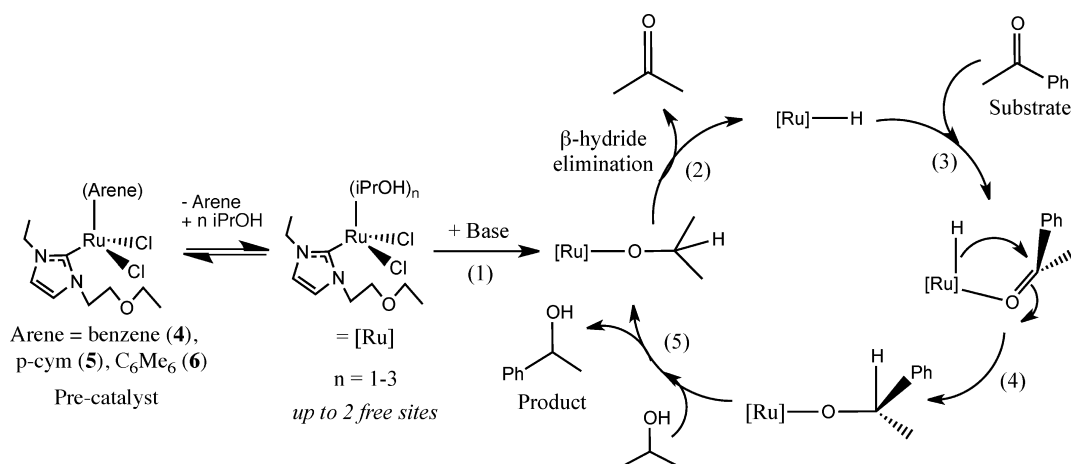


Figure 9. Proposed mechanism for the catalytic transfer hydrogenation of acetophenone to 1-phenylethanol in 2-propanol with catalysts 4–6.

occurred, then at 80 °C there is more ring-slipped arene than free arene present, suggesting that the *p*-cymene is still “partially” coordinated under typical catalysis conditions.

With complex 6, the signal for the methyl groups of coordinated hexamethylbenzene (δ 1.85) shifts downfield and splits and becomes two singlets upon the addition of KOH (Figure 7). As the temperature is increased, the two peaks begin to coalesce, and at 80 °C they collapse into a broad single peak. Free hexamethylbenzene (δ 2.09) appears at 60 °C (trace), and this peak increases slightly at 80 °C. The low intensity of free hexamethylbenzene and presence of the broad singlet at 80 °C suggests that, under reaction catalysis conditions, hexamethylbenzene ligand may undergo a ring slip and may still be coordinated.

The key observations from the variable-temperature ^1H NMR study with complexes 4–6 are summarized in Table 6. Benzene appears to be more labile than cymene, and hexamethylbenzene is the least labile. Under catalysis conditions (reflux, 85 °C), only complex 4 shows complete arene loss. Both 5 and 6 show spectra suggestive of ring-slipped arenes, with some partial decooordination of cymene and C_6Me_6 . When transfer hydrogenation was performed with catalyst 4 in the presence of excess free benzene (C/B/S/benzene = 1/25/200/1000), only 68% conversion of 1-phenylethanol was observed in the first hour. This conversion is substantially less than the 86% conversion observed in 1 h when no free arene is added to the reaction flask (Table 2, entry 9). All of these results support the trend that a greater extent of arene decooordination is correlated with higher catalytic activity.

Arene decooordination during catalysis has been discussed in the literature previously,^{82,83} but few studies have investigated how varying the arene impacts catalytic activity. Arene loss in Ru NHC complexes is observed for olefin hydrogenation with $\text{H}_2(\text{g})$, but these conditions are quite different than those employed here.⁴⁰ Similarly, Ru(arene) catalysts for propargylation⁸⁴ lose arene to form the active catalyst. Although other Ru(NHC)(arene) transfer hydrogenation catalysts appear in the literature to our knowledge this is the first detailed variable-temperature NMR study on the fate of the arene ligand in these catalysts.

Another interesting feature of the elevated temperature NMR spectra for 4–6 in 2-propanol- d_8 with base is the fate of the resonances for the NHC ligand. We do not see free imidazole or imidazolium salts present, but the ruthenium-

bound NHC signals are broadened at elevated temperatures, possibly due to dynamic exchange processes (Figures SI-24–SI-26, Supporting Information). The original NHC signals are split into multiple resonances, suggesting two species, perhaps due to formation of a hydride and/or 2-propoxide complex(es) (evidence described further below).

Variable-Temperature Studies of 4–6 in Basic 2-Propanol with Substrate. Tests were done to confirm that complexes 4–6 remain competent for the catalytic transfer hydrogenation when heated as described above (see Variable-Temperature Studies of 4–6 in Basic 2-Propanol without Substrate). A degassed reaction mixture identical with each described above was prepared, and after heating to 80 °C acetophenone was added. The product, 1-phenylethanol, was still produced with each catalyst, albeit with lower percent conversion (Table SI-2, Supporting Information). This decrease in conversion shows that the order in which reaction components are added (base is usually added last in most transfer hydrogenation experiments; see the Experimental Section) and/or the pressure of the reaction vessel (degassed vs under 1 atm of N_2) influence the yield of the reaction.

Additionally, a ^1H NMR experiment with 4 was performed exactly as shown in Figure 5, but with acetophenone present (4/KOH/acetophenone = 1/10/10; Figure 8). It was necessary to use 10 mol % of catalyst in order to observe the resonances for the catalyst, substrate, and product simultaneously. Again, as the temperature is raised, free benzene forms and coordinated benzene diminishes. As expected, the reaction proceeds very rapidly (reaction began at 25 °C upon adding base and was complete by the time of acquisition of the 60 °C spectrum) due to a 20-fold increase in mole percent of catalyst, in comparison to our experiments above with 0.5 mol % catalyst. Figure 8 shows that upon the addition of base the methyl singlet of acetophenone (δ 2.5) significantly broadens and forms several peaks; this may represent an acetophenone complex of ruthenium. Similarly, the broad resonance with multiple peaks (δ 2.0) in the 25 and 40 °C spectra may be coordinated acetone; this resonance sharpens with increasing temperature, and at higher temperature this peak is assigned to (mostly free) acetone (Figures 8 and Figures SI-24–SI-26 (Supporting Information)).⁸⁵ The base 2-propoxide (possibly coordinated to Ru) is expected to have methyl resonances in the δ 1.1 region, and these appear to be present, but this region is broad and obscured by 2-propanol; therefore, this assignment is

uncertain. Hydride ligands are not seen in these NMR spectra, perhaps due to line broadening; however, we have observed hydride signals with catalyst 7 under substrate-free conditions (see Transfer Hydrogenation of Acetophenone with Precatalysts 4–8 and Figure SI-21 (Supporting Information)).

Proposed Mechanism. The evidence presented herein shows that the apparent rate of transfer hydrogenation is proportional to how readily arene loss occurs. Therefore, we propose the mechanism for transfer hydrogenation with precatalysts 4–6 in Figure 9. Arene loss occurs, and solvent coordinates to produce a metal complex [Ru] with up to two free sites. [Ru] represents the active catalyst and includes NHC coordination, chloride ligands which are presumed to be bound (at least initially), though we have not investigated this point, and one to three solvent molecules. The addition of base can lead to a 2-propoxide complex by deprotonation or displacement of a 2-propanol ligand, as shown in step 1. The order of these initial steps is somewhat uncertain and is potentially dependent on what order reagents are added, which varies from our transfer hydrogenation to our variable-temperature studies. Step 2, β -hydride elimination, forms a hydride complex and is supported by the observation of hydride resonances from the reaction of 7 with base in methanol (see above and Figure SI-21 (Supporting Information)). This step also generates acetone, which may be coordinated prior to loss. For step 3 we propose acetophenone coordinates to the hydride complex; this hypothesis is supported by the observation of broad resonances at δ 2.5 that may indicate an acetophenone complex (discussed above). Hydride can then attack the α -C of the coordinated acetophenone, to give coordinated 1-phenylethoxide, as shown in step 4. Finally, in step 5, 2-propanol can displace and protonate 1-phenylethoxide to produce the product, 1-phenylethanol, and a 2-propoxide complex of [Ru] that can continue the cycle.

Our evidence suggests the slowest steps in this cycle may be arene loss and hydride attack on the carbonyl carbon. Arene loss may be incomplete in the case of more strongly donating arenes, and for these arenes (e.g. C_6Me_6) it is possible that the catalytic cycle proceeds through species with a ring-slipped arene rather than arene loss (though such a species is more electron rich and predicted to be a less effective catalyst). The influence of substrate electronic properties on the apparent rate suggests that a more electrophilic carbonyl group leads to faster hydride attack.

The mechanism in Figure 9 is consistent with our data and provides a proposal as to how arene lability can influence transfer hydrogenation rates. In view of this mechanism, it also makes sense that the hemilabile group, the ether group on the NHC ligand, has no impact on activity. As long as arene loss occurs to an adequate extent, 2-propanol solvent molecules can fill the vacant sites and provide a hemilabile (nonchelated) coordinating group, with as many as three coordination sites that are temporarily occupied by 2-propanol. We predict that hemilabile groups should have a greater impact on catalysis in noncoordinating solvents, but they are not beneficial with 2-propanol as the solvent in this study.

CONCLUSION

Ruthenium NHC complexes were used to probe how catalytic transfer hydrogenation is influenced by pendant ether groups, mono- or bis-NHC ligands, and arene ligands differing in lability and donor properties. It was found that the pendant ether groups do not appreciably influence catalytic transfer

hydrogenation (by comparison of 5 and 8), and while 4 was the most active catalyst in this study, most likely other (η^6 -benzene)Ru(NHC)Cl₂ complexes would perform similarly. While others have shown crystallographically that ether groups do coordinate to Ru and that O binding may stabilize coordinatively unsaturated species during catalysis,^{36,37} we saw no evidence for O (in 4–6) binding to the metal and enhancing catalytic rates in our studies. Arene lability has a great impact on catalysis, and benzene is the most labile arene employed in our studies. The need for generation of free sites is also evident from the superior performance of mono- over bis-NHC ligands. Attempts at catalyst poisoning with 1,10-phenanthroline and mercury have shown that the active catalyst appears to be homogeneous. While the exact identity of the active catalyst is uncertain, the evidence points to an NHC complex with 2-propanol/2-propoxide ligands that can generate a hydride catalyst in situ. The essential features for efficient transfer hydrogenation with ruthenium arene catalysts appear to include a labile arene ligand and a strong monodentate σ donor.

EXPERIMENTAL SECTION

General Considerations. All experiments involving ruthenium were carried out under an inert atmosphere using standard Schlenk line/glovebox techniques. Dichloromethane, ether, toluene, and hexanes were dried through an SPS system. MeOH was degassed and dried by distillation of a CaH₂–solvent mixture under reduced pressure and stored over molecular sieves. All ligand precursors were synthesized in air with solvents and reagents that were not further purified. Methylenebis(*N*-ethyl)imidazolium diiodide³⁸ was synthesized according to a known literature procedure. [RuCl₂(η^6 -C₆H₆)] was either synthesized according to a known literature procedure⁸⁶ or purchased. All other solvents and reagents were commercially available and were used without further purification. Glassware was dried in a 100 °C oven overnight prior to use. Proton and carbon NMR spectra were recorded using either a 300 MHz (300 MHz is the frequency for ¹H NMR spectra and 75 MHz for ¹³C NMR spectra on this instrument) or a 500 MHz (used primarily for ¹H NMR) Varian Unity Inova NMR spectrophotometer. Infrared spectra were collected on a Perkin-Elmer Spectrum One FT-IR spectrometer using a universal ATR sampling accessory. High-resolution (HR) mass spectrometry was performed on a VG70SE double-focusing, triple-quadrupole mass spectrometer equipped with FAB or CI ionization capability. Electrospray ionization (ESI) mass spectrometry was performed on a SCIEX API3000 mass spectrometer using 70/30 MeCN/H₂O with 0.1% TFA as a solubilizing agent and for fast atom bombardment (FAB, cesium ion). LIFDI-MS was performed at either University of California Riverside or University of Delaware. Elemental analysis was performed by Robertson Microlit, Ledgewood, NJ.

Synthesis of [Im^{Et,CH₂CH₂OEt}]⁺Br[−] (1). A mixture of 1-ethylimidazole (5.106g, 53.12 mmol) and BrCH₂CH₂OEt (8.350g, 54.98 mmol) was refluxed in 100 mL of toluene for 24 h. A sticky material was deposited at the bottom of the flask during refluxing, and the solution turned slightly brown. The contents were then cooled to −35 °C for 24 h, and the solvent was decanted off. The sticky material was washed with diethyl ether (~100 mL) and hexanes (~100 mL). The resulting viscous oil was dried under vacuum to afford [Im^{Et,CH₂CH₂OEt}]⁺Br[−] (1) in 52% yield (7.10 g, 0.0286 mol) (Im = imidazole derivative) without further purification. ¹H NMR (CDCl₃, 500 MHz): δ 1.09 (t, 3H, CH₃(OEt), ³J_{H-H} = 6.9 Hz), 1.55 (t, 3H, CH₃(NEt), ³J_{H-H} = 7.2 Hz), 3.44 (q, 2H, OCH₂, ³J_{H-H} = 6.9 Hz), 3.74 (t, 2H, OCH₂, ³J_{H-H} = 4.8 Hz), 4.36 (q, 2H, NCH₂, ³J_{H-H} = 7.5 Hz), 4.53 (t, 2H, NCH₂, ³J_{H-H} = 5.1 Hz), 7.53 (d, 1H, CH(Im), ³J_{H-H} = 1.5 Hz), 7.56 (d, 1H, CH(Im), ³J_{H-H} = 1.5 Hz), 10.21 (s, 1H, CH(Im)). ¹³C NMR (CDCl₃, 75 MHz): δ 14.46, 15.15 (2 × CH₃), 44.67, 49.29, 66.12, 67.63 (4 × CH₂), 121.46, 122.68 (2 × CH(Im)), 135.65

(NCHN(Im)). FAB MS: m/z 169.137 $[M]^+$ of cation (experimental), 169.134 $[M]^+$ (calculated).

Synthesis of 3-Ethyl-1-pentylimidazolium Bromide (3). Compound 3 was synthesized using a method similar to that described for 1 using 1-ethylimidazole (5.000 g, 52.01 mmol) and bromopentane (7.865 g, 52.07 mmol). 3-Ethyl-1-pentylimidazolium bromide (3) was obtained as a yellow, sticky oil in 90% yield (11.620 g, 47.22 mmol). ^1H NMR (CDCl_3 , 500 MHz): δ 0.52 (t, 3H, CH_3 , $^3J_{\text{H-H}} = 7.5$ Hz), 0.98 (m, 4H, $2 \times \text{CH}_2(\text{pentyl})$), 1.26 (t, 3H, CH_3 , $^3J_{\text{H-H}} = 7.5$ Hz), 1.59 (q, 2H, $\text{CH}_2(\text{pentyl})$, $^3J_{\text{H-H}} = 7.0$ Hz), 4.02 (t, 2H, NCH_2 , $^3J_{\text{H-H}} = 7.5$ Hz), 4.11 (q, 2H, NCH_2 , $^3J_{\text{H-H}} = 7.0$ Hz), 7.33 (d, 1H, CH(Im), $^3J_{\text{H-H}} = 1.0$ Hz), 7.49 (d, 1H, CH(Im), $^3J_{\text{H-H}} = 1.5$ Hz), 9.99 (s, 1H, CH(Im)); ^{13}C NMR (CDCl_3 , 75 MHz): δ 12.90, 14.89 ($2 \times \text{CH}_3$), 21.05, 27.23, 29.05, 44.20, 48.94 ($5 \times \text{CH}_2$), 121.49, 121.55 ($2 \times \text{CH(Im)}$), 135.19 (NCHN(Im)). CI MS: $m/z = 167.155595$ $[M]^+$ of cation (experimental), 167.154824 $[M]^+$ of cation (calculated).

Synthesis of $\text{Im}^{\text{Et,CH}_2\text{CH}_2\text{OEt}}\text{RuCl}_2(\text{benzene})$ (4). A mixture of 1 (0.201 g, 0.810 mmol) and Ag_2O (0.110, 0.473 mmol) in 20 mL of dichloromethane was stirred overnight under the exclusion of light. The solution was filtered, and $[\text{RuCl}_2(\text{benzene})]_2$ (0.204 g, 0.408 mmol) was added to the filtrate. The contents were further stirred for 20 h at room temperature. A white precipitate formed during the reaction, which was filtered off, and the solvent from the filtrate was dried under vacuum, leaving a dark orange solid, which was washed with 10 mL of hexanes and then dried under vacuum. The product was purified by recrystallization through dissolving in hot toluene and placing in a freezer at -35 °C. Crystals suitable for X-ray diffraction were grown by layering a dichloromethane solution with diethyl ether and storing at -35 °C to produce $\text{Im}^{\text{Et,CH}_2\text{CH}_2\text{OEt}}\text{RuCl}_2(\text{benzene})$ (4) as a dark orange solid in 68% yield (0.231 g, 0.552 mmol). ^1H NMR (CDCl_3 , 500 MHz): δ 1.17 (t, 3H, $\text{CH}_3(\text{OEt})$, $^3J_{\text{H-H}} = 7.2$ Hz), 1.42 (t, 3H, $\text{CH}_3(\text{NET})$, $^3J_{\text{H-H}} = 7.2$ Hz), 3.47 (m, br, 2H, OCH_2), 3.71 (m, br, 2H, OCH_2), 4.22 (m, br, 1H, NCH_2), 4.53 (m, br, 1H, NCH_2), 4.57 (m, br, 1H, NCH_2), 4.61 (m, br, 1H, NCH_2), 5.56 (s, 6H, (benzene)), 7.05 (d, 2H, CH(Im), $^3J_{\text{H-H}} = 2.4$ Hz), 7.31 (d, 1H, CH(Im), $^3J_{\text{H-H}} = 2.4$ Hz). ^{13}C NMR (CDCl_3 , 75 MHz): δ 15.40, 17.02 ($2 \times \text{CH}_3$), 46.35, 51.77, 66.73, 70.88 ($4 \times \text{CH}_2$), 86.44 (benzene), 121.36, 122.97 ($2 \times \text{CH(Im)}$), 171.73 ($\text{C}_{\text{carbene-Ru}}$). IR (ν , cm^{-1}): 3102 (C–H aromatic), 2966, 2878 (C–H sp^3), 1435, 1411, 1394, 1348, 1255, 1230, 1195 (weak), 1161 (weak), 1105, 1075, 1045, 921 (weak), 813, 740, 686. LIFDI MS: m/z 418.0 $[M]^+$ (experimental), 418.3 $[M]^+$ (calculated). FAB MS: m/z 383.046414 $[M - \text{Cl}]^+$ (experimental), 383.045274 $[M - \text{Cl}]^+$ (calculated). Anal. Calcd for $\text{C}_{15}\text{H}_{22}\text{ON}_2\text{Cl}_2\text{Ru}$: C, 43.06; H, 5.30; N, 6.70. Found: C, 42.78; H, 5.10; N, 6.58. See spectra in Figures SI-1–SI-4 (Supporting Information).

Synthesis of $\text{Im}^{\text{Et,CH}_2\text{CH}_2\text{OEt}}\text{RuCl}_2(p\text{-cymene})$ (5). Compound 5 was synthesized using a method similar to that described for 4 with 1 (0.209 g, 0.843 mmol), Ag_2O (0.101 g, 0.436 mmol), and $[\text{RuCl}_2(p\text{-cymene})]_2$ (0.258 g, 0.421 mmol). The product was purified by recrystallization through dissolving in hot toluene and placing in the freezer at -35 °C. Crystals suitable for X-ray diffraction were grown by dissolving in dichloromethane and layering with hexanes to produce $\text{Im}^{\text{Et,CH}_2\text{CH}_2\text{OEt}}\text{RuCl}_2(p\text{-cymene}) \cdot 0.9\text{H}_2\text{O}$ ($5 \cdot 0.9\text{H}_2\text{O}$) as an orange solid in 70% yield (0.281 g, 0.592 mmol). ^1H NMR (CDCl_3 , 500 MHz): δ 1.18 (t, 3H, $\text{CH}_3(\text{OEt})$, $^3J_{\text{H-H}} = 7.0$ Hz), 1.23 (d, 6H, $\text{CH}_3(i\text{Pr})$, $^3J_{\text{H-H}} = 6.5$ Hz), 1.45 (t, 3H, $\text{CH}_3(\text{NET})$, $^3J_{\text{H-H}} = 7.0$ Hz), 2.03 (s, 3H, $\text{CH}_3(\text{cymene})$), 2.91 (m, 1H, CH($i\text{Pr}$)), 3.48 (m, 2H, OCH_2), 3.71 (m, 2H, OCH_2), 4.07–4.23 (m, 2H, NCH_2), 4.73–4.80 (m, 2H, NCH_2), 5.12 (d, 2H, cymene), 5.40 (d, 2H, cymene), 7.03 (d, 1H, CH(Im), $^3J_{\text{H-H}} = 2.0$ Hz), 7.38 (d, 1H, CH(Im), $^3J_{\text{H-H}} = 2.0$ Hz). ^{13}C NMR (CDCl_3 , 75 MHz): δ 15.40, 17.05, 18.74, 22.76 ($4 \times \text{CH}_3$), 30.89 (CH($i\text{Pr}$)), 46.47, 51.80, 66.70, 71.25 ($4 \times \text{CH}_2$), 82.87, 85.14, 85.48, 99.81, 108.57 (cymene), 121.14, 123.33 ($2 \times \text{CH(Im)}$), 173.82 ($\text{C}_{\text{carbene-Ru}}$). IR (ν , cm^{-1}): 3094 (C–H aromatic), 2958, 2864 (C–H sp^3), 1455, 1413, 1377, 1346, 1255, 1196 (weak), 1124, 1108, 1077, 1045, 928 (weak), 868, 802, 733, 710, 689; LIFDI MS: m/z 474.3 $[M]^+$ (experimental), 474.4 $[M]^+$ (calculated). Anal. Calcd for $\text{C}_{19}\text{H}_{30}\text{ON}_2\text{Cl}_2\text{Ru}$: C, 48.10; H, 6.37; N, 5.90. Found: C, 47.35; H, 6.60; N, 5.83 (note that the hygroscopic nature of this molecule makes

it difficult to know how many waters of recrystallization are present, or if the sample crystallized without water in the lattice, and this can alter the analytical results). See spectra in Figures SI-5–SI-8 (Supporting Information).

Synthesis of $\text{Im}^{\text{Et,CH}_2\text{CH}_2\text{OEt}}\text{Ru}(\text{Cl})_2(\text{C}_6\text{Me}_6)$ (6). Compound 6 was synthesized by a method similar to that described for 4 using 1 (0.135 g, 0.544 mmol), Ag_2O (0.065, 0.280 mmol), and $[\text{RuCl}_2(\text{C}_6\text{Me}_6)]_2$ (0.176 g, 0.271 mmol). The product was purified by recrystallization through dissolving in hot toluene and placing in the freezer at -35 °C. The product was purified by recrystallization from dichloromethane and hexanes at room temperature to produce $\text{Im}^{\text{Et,CH}_2\text{CH}_2\text{OEt}}\text{RuCl}_2(\text{C}_6\text{Me}_6)$ (6) as an orange solid in 69% yield (0.188 g, 0.371 mmol). ^1H NMR (CDCl_3 , 500 MHz): δ 1.17 (t, 3H, $\text{CH}_3(\text{OEt})$, $^3J_{\text{H-H}} = 7.0$ Hz), 1.44 (t, 3H, $\text{CH}_3(\text{NET})$, $^3J_{\text{H-H}} = 6.5$ Hz), 1.98 (s, 18H, C_6Me_6), 3.46 (br, 2H, OCH_2), 3.74 (br, 2H, OCH_2), 3.85 (m, 2H, NCH_2), 4.64–4.85 (m, 2H, NCH_2), 6.99 (s, 2H, CH(Im)), 7.43 (s, 1H, CH(Im)). ^{13}C NMR (CDCl_3 , 75 MHz): δ 15.54, 15.78, 17.35 ($3 \times \text{CH}_3$), 46.05, 51.36, 66.60, 72.14 ($4 \times \text{CH}_2$), 93.88 (benzene), 121.15, 124.15 ($2 \times \text{CH(Im)}$), 176.82 ($\text{C}_{\text{carbene-Ru}}$). IR (ν , cm^{-1}): 2931, 2875 (C–H sp^3), 1431, 1408, 1393, 1376, 1344, 1248, 1217, 1197, 1167 (weak), 1110, 968 (weak), 949 (weak), 922 (weak), 804, 729, 712 (weak), 691. CI MS: m/z 502.107973 $[M]^+$ (experimental), 502.109167 $[M]^+$ (calculated). Anal. Calcd for $\text{C}_{21}\text{H}_{34}\text{ON}_2\text{Cl}_2\text{Ru}$: C, 50.20; H, 6.82; N, 5.58. Found: C, 50.89; H, 6.92; N, 5.50. See spectra in Figures SI-9–SI-12 (Supporting Information).

Synthesis of $\text{RuCl}(\text{methylenebis}(\text{Im}^{\text{Et}})_2)(\eta^6\text{-}p\text{-cymene})\text{PF}_6$ (7). Compound 7 was synthesized using a slightly modified literature procedure.⁴⁰ A mixture of methylenebis(*N*-ethyl)imidazolium diiodide (2.715 g, 5.888 mmol), Ag_2O (3.382 g, 14.72 mmol), and 100 mL of distilled water was mixed at room temperature with the exclusion of light for 30 min. A dark gray mixture formed, which was filtered through Celite to afford a clear solution. An aqueous solution of NH_4PF_6 (6.862 g, 42.10 mmol) was added to the filtrate to instantly produce a white precipitate. The precipitate was collected by vacuum filtration and washed with distilled water (2×320 mL) and diethyl ether (2×200 mL). The product was dried under vacuum. The formation of the silver NHC salt was verified by ^1H NMR in DMSO- d_6 . The yield of $[\text{Ag}^+\text{methylenebis}(\text{N-ethylIm})_2]\text{PF}_6$ was 1.591 g (3.489 mmol), and the percent yield was 59%.

The silver carbene salt (1.554 g, 3.408 mmol), $[(\eta^6\text{-}p\text{-cymene})\text{-RuCl}_2]_2$ (1.043 g, 1.703 mmol), and 100 mL of dichloromethane were stirred at room temperature for 18 h. The orange mixture was then filtered through Celite. The orange filtrate was collected, and the volume was reduced to 20 mL. $\text{RuCl}(\text{methylenebis}(\text{N-ethylIm})_2)(\eta^6\text{-}p\text{-cymene})^+\text{PF}_6^-$ (7) precipitated as a yellow solid upon the addition of 240 mL of diethyl ether. The product was collected by gravity filtration and dried under vacuum to produce $\text{RuCl}(\text{methylenebis}(\text{Im}^{\text{Et}})_2)(\eta^6\text{-}p\text{-cymene})\text{PF}_6$ (7) in 87% yield (1.834 g, 2.958 mmol). Crystals suitable for X-ray crystallography were grown in methanol at room temperature. ^1H NMR (CDCl_3 , 500 MHz): δ 1.05 (d, 6H, $\text{CH}_3(i\text{Pr})$, $^3J_{\text{H-H}} = 6.5$ Hz), 1.48 (t, 6H, $\text{CH}_3(\text{NET})$, $^3J_{\text{H-H}} = 7.0$ Hz), 2.13 (s, 3H, $\text{CH}_3(\text{cymene})$), 2.43 (m, 1H, CH($i\text{Pr}$)), 4.32 (m, 2H, $\text{CH}_2(\text{NET})$), 4.48 (m, 2H, $\text{CH}_2(\text{NET})$), 5.48 (d, 1H, NCH_2N , $^2J_{\text{H-H}} = 13.0$), 5.59 (d, 2H, cymene, $^3J_{\text{H-H}} = 6.5$ Hz), 5.64 (d, 2H, cymene, $^3J_{\text{H-H}} = 6.5$ Hz), 6.10 (d, 1H, NCH_2N , $^2J_{\text{H-H}} = 14.0$ Hz), 7.12 (d, 2H, CH(Im), $^3J_{\text{H-H}} = 1.5$ Hz), 7.33 (d, 2H, CH(Im), $^3J_{\text{H-H}} = 2.0$ Hz). ^{13}C NMR (CDCl_3 , 75 MHz): δ 16.4 (CH₃(NET)), 18.7 (CH₃($i\text{Pr}$)), 22.8 (CH($i\text{Pr}$)), 32.1 (CH₃(cymene)), 45.6 (CH₂(NET)), 61.6 (NCH₂N), 91.8, 86.6 ($2 \times \text{C}_{\text{cym-H}}$), 104.0, 108.4 ($2 \times \text{C}_{\text{cym-C}}$), 122.3, 121.2 ($2 \times \text{CH(Im)}$), 173.8 ($\text{C}_{\text{carbene-Ru}}$). IR (ν , cm^{-1}): 3100 (C–H aromatic), 2968 (C–H sp^3), 1472, 1423, 1357 (weak), 1259, 1214, 1180, 1053 (weak), 725 (strong), 731, 697, 686. MS (ESI): $[\text{C}_{21}\text{H}_{30}\text{N}_4\text{RuCl}]^+$ calculated $[M]$ m/z 475.1, experimental m/z $[M]$ 475.1. IR (cm^{-1}): 2968 (w), 3150 (w), 1472 (w), 1423 (w), 825 (s). Anal. Calcd for $\text{C}_{21}\text{H}_{30}\text{N}_4\text{ClF}_6\text{PRu}$: C, 40.64; H, 4.88; N, 9.03. Found: C, 40.58; H, 4.64; N, 8.74. See spectra in Figures SI-13–SI-16 (Supporting Information).

Synthesis of $\text{Im}^{\text{Et,Pentyl}}\text{RuCl}_2(p\text{-cym})$ (8). Compound 8 was synthesized using a method similar to that described for 4 using 3

(0.327 g, 1.329 mmol), Ag₂O (0.180, 0.784 mmol), and [RuCl₂(p-cymene)]₂ (0.400 g, 0.653 mmol). The product was purified by recrystallization through dissolving in hot toluene and placing in a freezer at -35 °C to produce Im^{Et,Pentyl}RuCl₂(p-cym) (**8**) as an orange solid in 68% yield (0.422 g, 0.893 mmol). Crystals suitable for X-ray diffraction were grown by dissolving in dichloromethane and layering with hexanes. ¹H NMR (CDCl₃, 500 MHz): δ 0.92 (t, 3H, CH₃(NPent)), ³J_{H-H} = 7.0 Hz), 1.24 (d, 6H, CH₃(iPr), ³J_{H-H} = 7.5 Hz), 1.37 (m, br, 4H, CH₂(NPent)), 1.45 (t, 3H, CH₃(NEt)), ³J_{H-H} = 7.3 Hz), 1.68 (br, 1H, CH₂(NPent)), 1.98 (br, 1H, CH₂(NPent)), 2.05 (s, 3H, CH₃(cymene)), 2.91 (m, 1H, CH(iPr)), 3.97 (br, m, 1H, NCH₂), 4.09 (br, m, 1H, NCH₂), 4.59 (br, m, 1H, NCH₂), 4.72 (br, m, 1H, NCH₂), 5.08 (d, 2H, cymene, ³J_{H-H} = 6.5 Hz), 5.38 (d, 2H, cymene, ³J_{H-H} = 6.0 Hz), 7.07 (d, 2H, CH(Im), ³J_{H-H} = 2.0 Hz), 7.08 (d, 2H, CH(Im), ³J_{H-H} = 2.0 Hz). ¹³C NMR (CDCl₃, 75 MHz): δ 14.2 (CH₃(NPent)), 14.3 (CH₃(NEt)), 17.1 (CH₂(NPent)), 18.8 (CH₃(cymene)), 22.8 (CH₃(iPr)), 29.2, 30.9 (2 × CH₂(NPent)), 31.8 (CH(iPr)), 46.4, 51.6 (2 × NCH₂), 83.0, 85.2 (2 × C_{cym-H}), 99.5, 108.2 (2 × C_{cym-C}), 121.5, 122.0 (2 × CH(Im)), 173.3 (C_{carbene-Ru}). IR (ν, cm⁻¹): 3057 (C-H aromatic), 2956, 2928, 2864 (C-H sp³), 1552 (weak), 1502, 1459, 1414, 1397, 1376, 1349, 1252, 1212, 1128, 1111, 1095, 1062, 1030, 1007 (weak), 954, 898, 868, 802, 747, 728, 687, 669; MS (Cl, CH₂Cl₂): m/z 472.0977 [M]⁺ (experimental), 472.0986 [M]⁺ (calculated). Anal. Calcd for C₂₀H₃₂N₂Cl₂Ru: C, 50.84; H, 6.83; N, 5.93. Found: C, 49.93; H, 6.43; N, 5.96. See spectra in Figures SI-17–SI-20 (Supporting Information).

General Procedure for Transfer Hydrogenation Studies. All experiments, unless otherwise stated, were carried out under an inert atmosphere using standard Schlenk line/glovebox techniques. Commercially available anhydrous 2-propanol was stored in a glovebox and used for all transfer hydrogenation reactions. Aliquot purification was done in open air with ether and hexanes that were used without any further purification.

In a typical run (Table 2), catalyst **4** (4 mg, 10.0 μmol) was added to a three-neck Schlenk flask by either direct addition of a weighed out aliquot or by addition as a 2.0 mL sample from a 0.005 M standard solution of catalyst in 2-propanol. Next, 1,3,5-trimethoxybenzene (111 mg, 0.667 mmol) and acetophenone (240 mg, 2.00 mmol) were added to the flask, which was attached to a reflux condenser and placed in an oil bath at 85 °C for 5 min. Next, KOtBu (0.028 g, 0.250 mmol) in 2-propanol (amount needed to bring total 2-propanol volume to 10 mL) was added to the mixture. Upon mixing, the solution became homogeneous.

At the desired sampling time, a 0.2 mL aliquot was drawn via a syringe and quenched in hexanes (2.0 mL). The mixture was filtered through a short stem pipet containing glass wool and a plug of Celite and then washed with ether (3 × 2 mL). The solvent was then gently removed from the filtrate under vacuum with little or no heat. The residue was dissolved in CDCl₃ and analyzed by ¹H NMR. Percent conversions were determined by comparing the integration of the methyl protons of the alcohol with the methoxy protons of the internal standard.

High-Temperature NMR Experiment. All measurements were made on a 500 MHz Varian Unity Inova NMR spectrophotometer. Inside a nitrogen glovebox an NMR tube containing ruthenium precatalyst (10 μmol), 1,3,5-trimethoxybenzene as internal standard (5 mg, 29.7 μmol), and 1.0 mL of 2-propanol-*d*₈ was prepared. The tube was sealed in order to avoid air contamination, and a ¹H NMR spectrum was recorded. Next, the tube was brought back into the glovebox and KOH (5 mg, 89.1 μmol) was added. Outside of the glovebox the solvent was degassed by three freeze–pump–thaw cycles, and the tube was flame-sealed. ¹H NMR spectra were taken at 25, 40, 60, 70, and 80 °C. All spectra were referenced to the methoxy protons (δ 3.62 ppm) of the internal standard.

■ ASSOCIATED CONTENT

Supporting Information

Figures, tables, and CIF files giving spectra of complexes **4–8**, spectra of the Ru hydride complex formed from **7**, additional

structural figures for **4**, **5**, and **8**, additional transfer hydrogenation results related to mercury test and variable-temperature NMR studies, full variable-temperature NMR spectra of Ru complexes **4–6**, and X-ray crystallographic data for complexes **4**, **5**, **7**, and **8**. This material is available free of charge via the Internet at <http://pubs.acs.org>.

■ AUTHOR INFORMATION

Notes

The authors declare no competing financial interest.

■ ACKNOWLEDGMENTS

We are grateful for financial support from the NSF CAREER (Grant CHE-0846383), ACS-PRF (Grant 48295-AC3), and Drexel University. The diffractometer was funded by NSF grant 0087210, by Ohio Board of Regents Grant CAP-491, and by YSU. We also thank Tim Wade (Drexel University) for MS analysis. We thank John Dykins (University of Delaware) and Richard Kondrat (University of California, Riverside) for performing LIFDI MS experiments. A Drexel University Career Development award funded travel to seminars and conferences to discuss this project with colleagues, and in particular our discussions with Marcetta Y. Darensbourg were helpful. We also thank Jack R. Norton and Anthony W. Addison for helpful discussions. Finally, we thank the members of the Papish research group for assistance and suggestions.

■ REFERENCES

- (1) Ikariya, T.; Murata, K.; Noyori, R. *Org. Biomol. Chem.* **2006**, *4*, 393–406.
- (2) Nieto, I.; Livings, M. S.; Sacchi, J. B., III; Reuther, L. E.; Zeller, M.; Papish, E. T. *Organometallics* **2011**, *30*, 6339–6342.
- (3) Noyori, R.; Hashiguchi, S. *Acc. Chem. Res.* **1997**, *30*, 97–102.
- (4) Blaser, H. - U.; Malan, C.; Pugin, B.; Spindler, F.; Steiner, H.; Studer, M. *Adv. Synth. Catal.* **2003**, *345*, 103–151.
- (5) Clapham, S. E.; Hadzovic, A.; Morris, R. H. *Coord. Chem. Rev.* **2004**, *248*, 2201–2237.
- (6) Papish, E. T.; Rix, F. C.; Spetseris, N.; Norton, J. R.; Williams, R. D. *J. Am. Chem. Soc.* **2000**, *122*, 12235–12242.
- (7) Papish, E. T.; Magee, M. P.; Norton, J. R. Protonation of Transition Metal Hydrides to Give Dihydrogen Complexes: Mechanistic Implications and Catalytic Applications. In *Recent Advances in Hydride Chemistry*; Elsevier: Amsterdam, 2001; pp 39–74.
- (8) Corberan, R.; Mas-Marza, E.; Peris, E. *Eur. J. Inorg. Chem.* **2009**, 2009, 1700–1716.
- (9) Mata, J. A.; Poyatos, M.; Peris, E. *Coord. Chem. Rev.* **2007**, *251*, 841–859.
- (10) Hahn, F. E.; Jahnke, M. C. *Agnew. Chem. Int. Ed.* **2008**, *47*, 3122–3172.
- (11) Diez-Gonzalez, S.; Marion, N.; Nolan, S. P. *Chem. Rev.* **2009**, *109*, 3612–3676.
- (12) Peris, E.; Crabtree, R. H. *Coord. Chem. Rev.* **2004**, *248*, 2239–2246.
- (13) Diez-Gonzalez, S.; Nolan, S. P. *Coord. Chem. Rev.* **2007**, *251*, 874–883.
- (14) Droge, T.; Glorius, F. *Agnew. Chem. Int. Ed.* **2010**, *49*, 6940–6952.
- (15) Jahnke, M. C.; Hahn, F. E. Introduction to N-Heterocyclic Carbenes: Synthesis and Stereoelectronic Parameters. In *N-Heterocyclic Carbenes from Laboratory Curiosities to Efficient Synthetic Tools*; Royal Society of Chemistry: Cambridge, U.K., 2011; RSC Catalysis Series Vol. 6, pp 1–41.
- (16) Normand, A. T.; Cavell, K. J. *Eur. J. Inorg. Chem.* **2008**, 2008, 2781–2800.
- (17) Dragutan, V.; Dragutan, I.; Delaube, L.; Demonceau, A. *Coord. Chem. Rev.* **2007**, *251*, 765–794.

- (18) Yigit, M.; Yigit, B.; Ozdemir, I.; Cetinkaya, E.; Cetinkaya, B. *Appl. Organomet. Chem.* **2006**, *20*, 322–327.
- (19) O, W. W. N.; Lough, A. J.; Morris, R. H. *Organometallics* **2009**, *28*, 6755–6761.
- (20) Horn, S.; Albrecht, M. *Chem. Commun.* **2011**, *47*, 8802–8804.
- (21) Gnanamgari, D.; Sauer, E. L. O.; Schley, N. D.; Butler, C.; Incarvito, C. D.; Crabtree, R. H. *Organometallics* **2009**, *28*, 321–325.
- (22) Fekete, M.; Joo, F. *Collect. Czech. Chem. Commun.* **2007**, *72*, 1037–1045.
- (23) Poyatos, M.; Maise-Francois, A.; Bellemin-Lapponaz, S.; Peris, E.; Gade, L. H. *J. Organomet. Chem.* **2006**, *691*, 2713–2720.
- (24) Enthaler, S.; Jackstell, R.; Hagemann, B.; Junge, K.; Erre, G.; Beller, M. *J. Organomet. Chem.* **2006**, *691*, 4652–4659.
- (25) DePasquale, J.; White, N. J.; Ennis, E. J.; Zeller, M.; Foley, J. P.; Papish, E. T. *Polyhedron* **2012**, DOI: 10.1016/j.poly.2012.10.010.
- (26) Horn, S.; Gandolfi, C.; Albrecht, M. *Eur. J. Inorg. Chem.* **2011**, 2863–2868.
- (27) Sanz, S.; Azua, A.; Peris, E. *Dalton Trans.* **2010**, *39*, 6339–6343.
- (28) Bassetti, M. *Eur. J. Inorg. Chem.* **2006**, 4473–4482.
- (29) Shaffer, A. R.; Schmidt, J. A. R. *Organometallics* **2009**, *28*, 2494–2504.
- (30) Yang, X.; Fei, Z.; Geldbach, T. J.; Phillips, A. D.; Hartinger, C. G.; Li, Y.; Dyson, P. J. *Organometallics* **2008**, *27*, 3971–3977.
- (31) Ohta, H.; Fujihara, T.; Tsujo, Y. *Dalton Trans.* **2008**, *3*, 379–385.
- (32) Turkmen, H.; Pape, T.; Hahn, F. E.; Cetinkaya, B. *Eur. J. Inorg. Chem.* **2008**, 5418–5423.
- (33) Binobaid, A.; Iglesias, M.; Beetstra, D.; Dervisis, A.; Fallis, I.; Cavell, K. J. *Eur. J. Inorg. Chem.* **2010**, 5426–5431.
- (34) Gulcernal, S.; Daran, J. C.; Cetinkaya, B. *Inorg. Chim. Acta* **2011**, *365*, 264–268.
- (35) Jimenez, M. V.; Fernandez-Tornos, J.; Perez-Torrente, J. J.; Modrego, F. J.; Winterle, S.; Cunchillos, C.; Lahoz, F. J.; Oro, L. A. *Organometallics* **2011**, *30*, 5493–5508.
- (36) Lund, C. L.; Sgro, M. J.; Cariou, R.; Stephan, D. W. *Organometallics* **2012**, *31*, 802–805.
- (37) Lund, C. L.; Sgro, M. J.; Stephan, D. W. *Organometallics* **2012**, *31*, 580–587.
- (38) Albrecht, M.; Miecznikowski, J. R.; Samuel, A.; Faller, J. W.; Crabtree, R. H. *Organometallics* **2002**, *21*, 3596–3604.
- (39) Liu, W.; Bendorf, K.; Proetto, M.; Abram, U.; Adelheid, H.; Gust, R. *J. Med. Chem.* **2011**, *54*, 8605–8615.
- (40) Gandolfi, C.; Heckenroth, M.; Neels, A.; Laurenczy, G.; Albrecht, M. *Organometallics* **2009**, *28*, 5112–5121.
- (41) Waller, M. P.; Robertazzi, A.; Platts, J. A.; Hibbs, D. E.; Williams, P. A. *J. Comput. Chem.* **2006**, *27*, 491–504.
- (42) Kim, J.-W.; Kim, J.-H.; Lee, D.-H.; Lee, Y.-S. *Tetrahedron Lett.* **2006**, *47*, 4745–4748.
- (43) Bauer, E. B.; Andavan, G. T. S.; Hollis, T. K.; Rubio, R. J.; Cho, J.; Kuchenbeiser, G. R.; Helgert, T. R.; Letko, C. S.; Tham, F. S. *Org. Lett.* **2008**, *10*, 1175.
- (44) Kumar, M.; Papish, E. T.; Zeller, M.; Hunter, A. D. *Dalton Trans.* **2010**, *39*, 59–61.
- (45) Kumar, M.; Papish, E. T.; Zeller, M.; Hunter, A. D. *Dalton Trans.* **2011**, *40*, 7517–7533.
- (46) Tenn, W. J., III; Conley, B. L.; Bischof, S. M.; Periana, R. A. *J. Organomet. Chem.* **2012**, *696*, 551.
- (47) Conde, A.; Fandos, R.; Hernandez, C.; Otero, A.; Rodriguez, A.; Ruiz, M. J. *Chem. Eur. J.* **2012**, *18*, 2319.
- (48) Canivet, J.; Suess-Fink, G. *Green Chem.* **2007**, *9*, 391.
- (49) Aranyos, A.; Csjernyik, G.; Szabo, K. J.; Backvall, J. E. *Chem. Commun.* **1999**, 351–352.
- (50) Samec, J. S. M.; Backvall, J. E.; Andersson, P. G.; Brandt, P. *Chem. Soc. Rev.* **2006**, *35*, 237–248.
- (51) Ouali, A.; Majoral, J. P.; Caminade, A. M.; Taillefer, M. *ChemCatChem* **2009**, *1*, 504–509.
- (52) Hagen, J. In *Industrial Catalysis: A Practical Approach*, 2nd ed.; Wiley-VCH: Weinheim, Germany, 2006.
- (53) Wettergren, J.; Zaitsev, A. B.; Adolfsson, H. *Adv. Synth. Catal.* **2007**, *349*, 2556–2562.
- (54) Han, M. L.; Hu, X. P.; Huang, J. D.; Chen, L. G.; Zheng, Z. *Tetrahedron: Asymmetry* **2011**, *22*, 222–225.
- (55) Ahlford, K.; Livendahl, M.; Adolfsson, H. *Tetrahedron: Asymmetry* **2009**, *50*, 6321–6324.
- (56) Baratta, W.; Siega, K.; Rigo, P. *Chem. Eur. J.* **2007**, *13*, 7479–7486.
- (57) Torres, J.; Sepulveda, F.; Carrion, M. C.; Jalon, F. A.; Manzano, B. R.; Rodriguez, A. M.; Zirakzadeh, A.; Weissensteiner, W.; Mucientes, A. E.; Angeles de la Pena, M. *Organometallics* **2011**, *30*, 3490–3503.
- (58) Carrion, M. C.; Sepulveda, F.; Jalon, F. A.; Manzano, B. R. *Organometallics* **2009**, *28*, 3822–3833.
- (59) Soriano, M. L.; Jalon, F. A.; Manzano, B. R.; Maestro, M. *Inorg. Chim. Acta* **2009**, *362*, 4486–4492.
- (60) Corberan, R.; Peris, E. *Organometallics* **2008**, *27*, 1954–1958.
- (61) Castarlenas, R.; Esteuruelas, M. A.; Onate, E. *Organometallics* **2008**, *27*, 3240–3247.
- (62) Lagaditis, P. O.; Lough, A. J.; Morris, R. H. *J. Am. Chem. Soc.* **2011**, *133*, 9662–9665.
- (63) Abdur-Rashid, K.; Clapham, S. E.; Hadzovic, A.; Harvey, J. N.; Lough, A. J.; Morris, R. H. *J. Am. Chem. Soc.* **2002**, *124*, 15104–15118.
- (64) Dong, Z. R.; Li, Y. Y.; Chen, J. S.; Li, B. Z.; Xing, Y.; Gao, J. X. *Org. Lett.* **2005**, *7*, 1043–1045.
- (65) Guan, H.; Iimura, M.; Magee, M. P.; Norton, J. R.; Zhu, G. J. *Am. Chem. Soc.* **2005**, *127*, 7805–7814.
- (66) Magee, M. P.; Norton, J. R. *J. Am. Chem. Soc.* **2001**, *123*, 1178–1179.
- (67) Ohkuma, T.; Koizumi, M.; Munz, K.; Hilt, G.; Kabuto, C.; Noyori, R. *J. Am. Chem. Soc.* **2002**, *124*, 6508–6509.
- (68) Dahlenburg, L.; Gotz, R. *Inorg. Chim. Acta* **2004**, *357*, 2875–2880.
- (69) Cadierno, V.; Crochet, P.; Diez, J.; Garcia-Garrido, S. E.; Gimeno, J. *Organometallics* **2004**, *23*, 4836–4845.
- (70) Murata, K.; Noyori, R.; Ikariya, T. *J. Org. Chem.* **1999**, *64*, 2186–2187.
- (71) Haack, K.-J.; Hashiguchi, S.; Fujii, A.; Ikariya, T.; Noyori, R. *Angew. Chem., Int. Ed.* **1997**, *36*, 285.
- (72) Mascarenhas, C. M.; Duffey, M. O.; Liu, S. Y.; Morken, J. P. *Org. Lett.* **1999**, *1*, 1427–1429.
- (73) Grabulosa, A.; Mannu, A.; Alberico, E.; Denurra, S.; Gladiali, S.; Muller, G. *J. Mol. Catal. A: Chem.* **2012**, *363–364*, 49–57.
- (74) Grabulosa, A.; Mannu, A.; Mezzetti, A.; Muller, G. *J. Organomet. Chem.* **2012**, *696*, 4221–4228.
- (75) Foley, P.; DiCosimo, R.; Whitesides, G. M. *J. Am. Chem. Soc.* **1980**, *102*, 6713–6725.
- (76) Anton, D. R.; Crabtree, R. H. *Organometallics* **1983**, *2*, 855–859.
- (77) Eberhard, M. R. *Org. Lett.* **2004**, *6*, 2125–2128.
- (78) Widegren, J. A.; Finke, R. G. *J. Mol. Catal. A: Chem.* **2003**, *198*, 317–341.
- (79) Bayram, E.; Linehan, J. C.; Fulton, J. L.; Roberts, J. A. S.; Szymczak, N. K.; Smurthwaite, T. D.; Ozkar, S.; Balasubramanian, M.; Finke, R. G. *J. Am. Chem. Soc.* **2011**, *133*, 18889–18902.
- (80) Bayram, E.; Finke, R. G. *ACS Catal.* **2012**, *2*, 1967–1975.
- (81) Darensbourg, M. Y.; Muetterties, E. L. *J. Am. Chem. Soc.* **1978**, *100*, 7425.
- (82) Solvhoj, A.; Madsen, R. *Organometallics* **2011**, *30*, 6044–6048.
- (83) Maggi, A.; Madsen, R. *Organometallics* **2012**, *31*, 451–455.
- (84) Bustelo, E.; Dixneuf, P. H. *Adv. Synth. Catal.* **2007**, *349*, 933–942.
- (85) The interpretation of the resonances at δ 2.5 and 2.0 is complicated by H/D coupling and H/D exchange, since KOH was used with 2-propanol- d_6 . This issue is unavoidable, as even if KOD were used, exchange with the protio substrate could occur.
- (86) Zhu, B.; Ellern, A.; Sygula, A.; Sygula, R.; Angelici, R. J. *Organometallics* **2007**, *26*, 1721–1728.